Research Article | Vol. 28, No. 18 / 31 August 2020 / Optics Express 26407
Optics EXPRESS

Pupil plane actuated remote focusing for rapid focal depth control

ZONGYUE CHENG,[1,2] HEHAI JIANG,[1,3] WENBIAO GAN,[2] AND MENG CUI[1,3,4,*]

[1]Bindley Bioscience Center, Purdue University, West Lafayette, IN 47907, USA
[2]Skirball Institute, Department of Neuroscience and Physiology, Department of Anesthesiology, New York University School of Medicine, New York, NY 10016, USA
[3]School of Electrical and Computer Engineering, Purdue University, West Lafayette, IN 47907, USA
[4]Department of Biology, Purdue University, West Lafayette, IN 47907, USA
*mengcui@purdue.edu

Abstract: Laser scanning is widely employed in imaging and material processing. Common laser scanners are often fast for 2D transverse scanning. Rapid focal depth control is highly desired in many applications. Although remote focusing has been developed to achieve fast focal depth control, the implementation is limited by the laser damage to the actuator near laser focus. Here, we present a new method named pupil plane actuated remote focusing, which enables sub-millisecond response time while avoiding laser damage. We demonstrate its application by implementing a dual-plane two-photon laser scanning fluorescence microscope for *in vivo* recording of calcium transient of neurons in mouse neocortex.

1. Introduction

Laser scanning is widely employed in many key areas. In material processing [1], laser scanning based material cutting and engraving has been routinely used to achieve high dimension accuracy and tight tolerance [2]. In additive manufacturing [3], laser scanning based 3D printing has been commercialized for a broad range of materials. In medicine, laser scanning has been applied to vision correction [4] and endoscopic imaging [5]. In biology, laser scanning serves as the foundation for a variety of 3D imaging technologies [6–12]. Thus, the advances of laser scanning method can broadly benefit many disciplines.

Common laser scanners such as polygon scanners and galvo scanners only implement fast transverse scanning [13,14]. The axial scan typically involves mechanical adjustment of the focusing lenses and is therefore very slow. To achieve faster axial scanning, a variety of solutions have been developed, such as liquid lens cells [15,16], ultrasonic lenses [17,18], holographic wavefront control [19–21], remote focusing [22,23], etc. Liquid lens cell has its advantage of simplicity and low cost. Mechanical lens surface deformation can achieve focal depth control at ~100 Hz rate. A major issue of liquid lens is the spherical aberration. The ideal defocusing wavefront, $ndcos(\theta)$ where n is the index of refraction, d is the defocusing distance and θ is the angle of incidence, depends on the numerical aperture (NA) of the objective lens [22]. As the majority of the objective lens design is based on the Abbe sine condition, the pupil plane spatial profile has nonlinear dependence on $cos(\theta)$. Therefore, the wavefront profiles for lenses of different NA are unlike. The mismatch between the liquid lens wavefront and the ideal defocusing wavefront leads to aberration (greater focal volume and reduced peak intensity). Ultrasonic lenses rely on the acoustic wave induced refractive index change to achieve high-speed (100 kHz – 1 MHz) focus tuning, which is faster than most scanners. However, similar to the liquid lens cell, it also suffers from spherical aberration [17]. For aberration free defocusing, holographic wavefront control has been utilized [20,21,24–27]. Deformable mirrors or spatial light modulators (SLM) can be employed to generate the desired defocusing wavefront. Residual

#402787 https://doi.org/10.1364/OE.402787
Journal © 2020 Received 14 Jul 2020; revised 6 Aug 2020; accepted 9 Aug 2020; published 21 Aug 2020

Optics EXPRESS

system aberration can also be corrected [19]. For long defocusing range, SLM is the preferred solution for its ample degrees of freedom with up to ~200 Hz update rate. However, each update is only for a defined defocusing distance. For a continuous axial scanning (e.g. over a range of ~200 focal locations), the scan rate will be quite slow (e.g., 1 Hz with a 200 Hz SLM). The development of remote focusing nicely solved these problems [22,23]. Using a pair of objective lenses of identical defocusing wavefront profiles and telecentric tube lenses, remote focusing can nicely relay the focal movement from one lens to the other. To achieve fast defocusing control, a galvanometer actuated miniature mirror was placed near the focal plane of the proximal objective, which enabled sub-millisecond step response time and kHz rate continuous scanning. A limitation for practical implementation is its power handling capability. In comparison, the liquid lens cells, ultrasonic lenses and holographic wavefront control all operate in the pupil plane, where the power density is well below that of the focal plane. Such a design has enabled the operation of high peak intensity lasers for both imaging and material processing. For remote focusing, the focusing actuator is located near the focal plane where the peak intensity is high, which could lead to damage to the optical surface. Therefore, the focal plane actuation design of remote focusing hindered the applications with high peak laser intensity despite its advantages of low aberration and high speed.

To enable a high-speed focal depth control without laser damage to the system, we have developed a new method, named pupil plane actuated remote focusing (PRF). The idea is to have two opposing objective lenses with their optical axes tilted with respect to each other (Fig. 1). We will use a high NA objective lens as the input lens such that it can provide sufficient solid angle to match that of the tilted output lens. In this way, the transverse movement of the input laser focus on its focal plane (Δy_0 in Fig. 1) can be decomposed into the axial (Δz) and the transverse movement (Δy) of the output laser focus. With such a configuration, the focal depth control can be implemented by a galvo at the pupil plane of the input lens where the laser beam is large and the laser intensity is low. As the common applications of laser scanning already include a transverse 2D scanner, the transverse movement (Δy) coupled with the axial scanning can be canceled by the 2D scanner to form purely axial scanning. From the perspective of degrees of freedom, we will only use three galvos to achieve fast arbitrary 3D positioning, e.g. one for y and z, one for x and one for y.

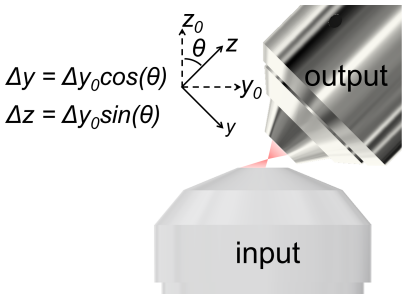

Fig. 1. Objective lens configuration for pupil plane actuated remote focusing.

2. Methods

We implemented the PRF module with an output NA of 0.8 and combined it with a two-photon laser (930 nm, 140 fs) scanning fluorescence microscope (Fig. 2(a)), which allowed us to quantify its spatial resolution and explore its neuroscience applications. We employed an NA 1.4 oil immersion objective as the input lens and an NA 0.8 water dipping objective as the output lens. The optical axis of the NA 0.8 objective was tilted by 45 degree from that of the NA 1. 4 lens. At

Optics EXPRESS

NA 0.8, the solid angle was 37 degree in water. With the additional 45 degree tilting, the largest angle was 82 degree, corresponding to a maximum input NA of 1.317, which was supported by the NA 1.4 input lens. The input lens required a cover slip, which was positioned by a linear stage (UMR5.16, Newport) such that the optical focus was on the surface between the cover slip and water. Experimentally, we used a 3-axis stage (9062-XYZ, Newport) to position the NA 0.8 objective such that its output beam was collimated along its optical axis. We further adjusted the cover slip position so that the beam profile was round and uniform. Scanning with the single-axis galvo 1 would shift the laser focus transversely on the focal plane of the input lens, which was projected into the transverse and the axial focus scanning of the output lens. Galvo 2 provided 2-axis transverse scanning. The collective control of these three scanning axes (three degrees of freedom) allowed us to achieve fast (130 µs small-step and 500 µs large-step response time) 3D focus control.

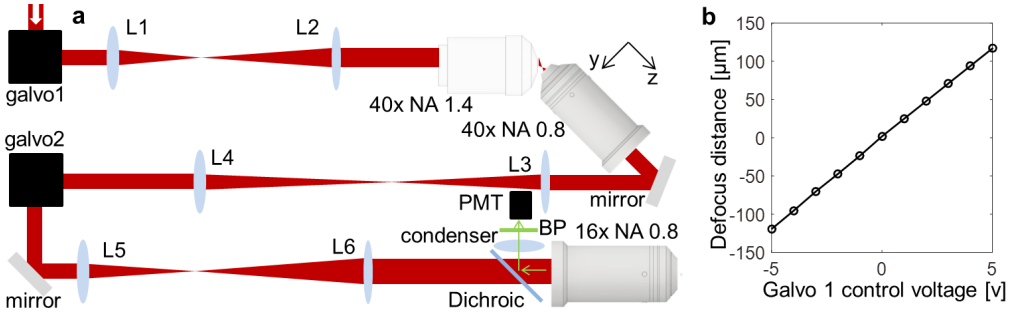

Fig. 2. (a) System design for PRF based two-photon laser scanning fluorescence microscope. Galvo1, single axis galvo scanner (8315k Cambridge Technology); L1-6, achromatic telecentric relay lenses with focal length 125, 300, 300, 187.5, 125, and 500 mm; Galvo2, two-axis galvo scanner (8315k Cambridge Technology); BP, bandpass filter (535/150 Semrock). (b) Defocus distance's dependence on galvo 1 voltage.

For two-photon imaging, we employed the scanimage software [14] for image recording. To flexibly shift the image location in 3D, we combined the scanimage galvo control analog signals with *xy* offset signals using analog signal summing amplifiers (SIM980, SRS). The three analog control signals, one for galvo1 and two for *xy* offset allowed us to achieve 3D positioning. In this work, we utilized the PRF to implement a dual-plane calcium imaging, in which we switched the imaging between two axial locations. To synchronize the image recording with the focal depth switching, we utilized the frame trigger offered by scanimage to update the signal to galvo1 and the offset signal to the *y* axis of galvo 2.

To calibrate the axial scan range and the *y* offset value that was needed to form purely axial scanning, we immobilized 0.2 µm diameter fluorescence beads (F8811, ThermoFisher) in 2% agar and positioned the agar sample using a precision linear stage (VP-25XA, Newport). After applying different voltage value to galvo 1, we controlled the vertical axis of the linear stage such that the same beads were back in focus. The stage reading allowed us to determine the axial shift (Fig. 2(b)). Next, we adjusted the *y* offset value of galvo 2 such that the beads returned to their original location on the image, which allowed us to determine the *y* offset values for achieving purely axial shift.

To evaluate the system performance for *in vivo* calcium imaging, we used 2-mouth old wild-type C57BL/6 mice which were injected with 200-300 nl AAV1-*Syn*-GCaMP6s-WPRE-SV40 (100843-AAV1, Addgene) in the primary sensory cortex 14 days before the imaging. We surgically removed the skull and implanted a 3 mm diameter No. 0 cover glass as the cranial

Optics EXPRESS

window. During the imaging, calcium data were collected from layer 1 and 2/3 of the primary sensory cortex. Changes of fluorescence normalized by the baseline fluorescence level ($\Delta F/F$) were quantified from regions of interest (ROI). The minimum 10% of each cell's fluorescence was defined as the baseline value (F) [28].

3. Results

We employed 0.2 μm diameter fluorescence beads to characterize the spatial resolutions (Fig. 3) over a defocusing range of ~240 μm. At each defocusing value, we recorded a 3D stack with 0.8 μm axial spacing, which allowed us to extract the spatial resolutions. Within a range of 200 μm, the transverse resolutions were rather consistent while the axial resolution varied (3-6 μm), which was nonetheless adequate for imaging neuronal somata and dendrites.

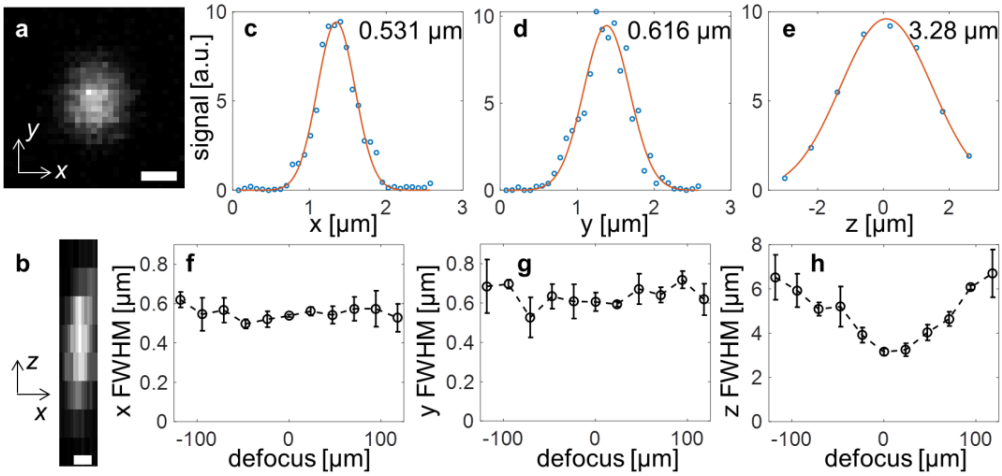

Fig. 3. Spatial resolution characterized by two-photon imaging of 0.2 μm beads. (a, b) Transverse and axial cross-section images with 0 defocusing. Scale bar, 0.5 μm. (c-e) Gaussian fitting with the full width at half maximum (FWHM) value shown. (f-h) Focus FWHM as a function of defocusing distance.

We employed the PRF system for dual-plane *in vivo* calcium imaging of neuronal activity in the awake mouse brain (Fig. 4). With the kHz non-resonant galvo scanner, we set the line rate to 1 kHz. With 240 lines per image, the frame rate was ~4 Hz. With the PRF based focal plane switching, we used the odd number frames to record at focal plane 1 (cerebral layer 1) and even number frames to record at focal plane 2 (cerebral layer 2/3). The axial separation between the two planes was ~200 μm (Fig. 4). To compensate for the tissue scattering induced focus intensity difference, we also dynamically (based on the scanimage frame trigger) adjusted the driving signal of the power control EO modulator (350-80-LA-BK, Conoptics). The average imaging power was 12 mW and 20 mW for plane 1 and 2, respectively. The animal was fully awake during the imaging. The spontaneous calcium transients from somata, dendrites and dendritic trunks were extracted from the time-lapse imaging (Figs. 4(b)–4(e)).

Optics EXPRESS

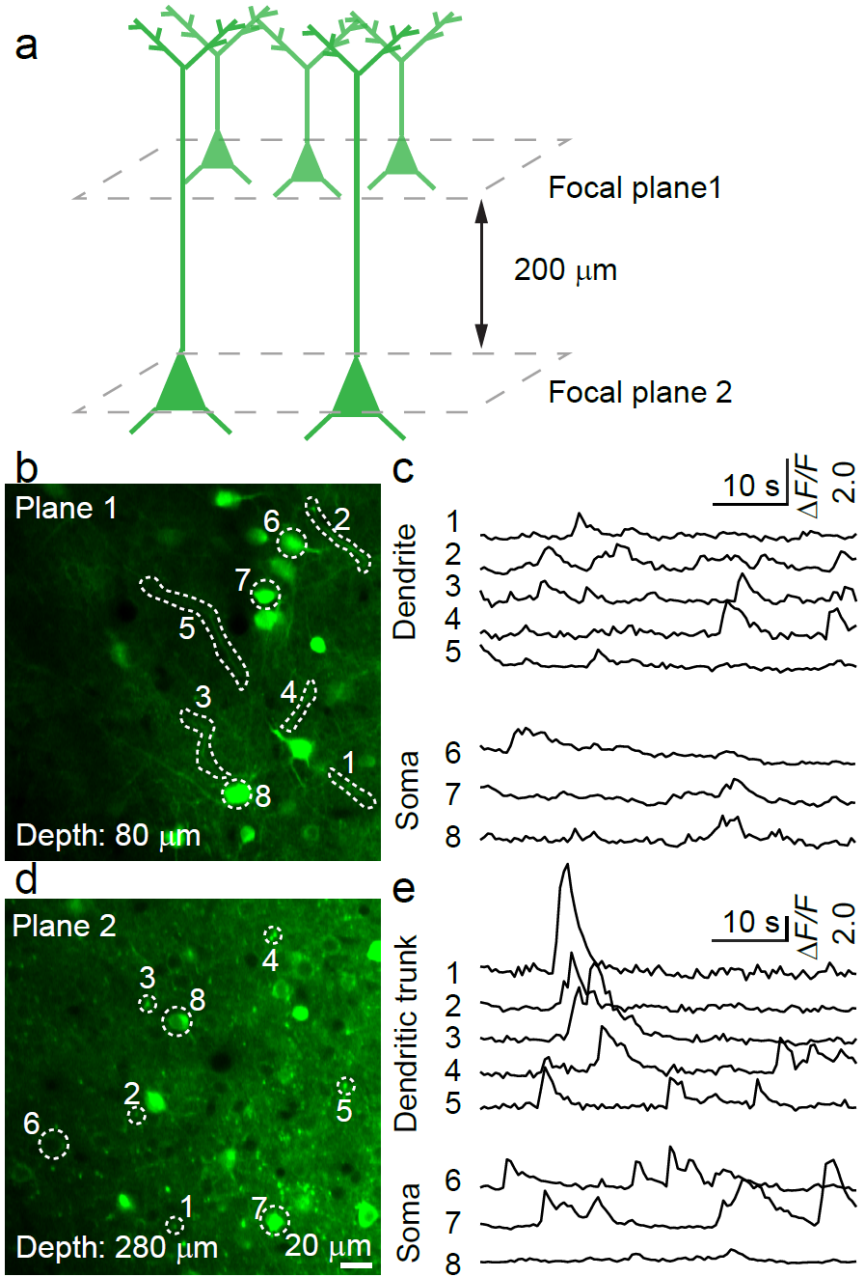

Fig. 4. Dual-plane *in vivo* calcium recording of neuronal activity in awake mouse brain. (a) Spatial configuration of the two imaging planes. (b, c) Image and calcium transients of dendrites and somata in the upper plane. (d, e) Image and calcium transients of dendritic trunks and somata in the lower plane.

Optics EXPRESS

4. Discussion

The key advantage of PRF is the greatly improved power handling capability. In conventional remote focusing systems, to fully utilize the scan range, the actuator needs to travel across the focal plane to access both the positive and the negative defocusing regions. Even if the focal plane can be avoided, the laser spot size on the actuator ranges from tens to a few hundred microns. In comparison, with PRF, the laser spot size on the actuator (galvo) ranges from several millimeters to above centimeter. Given the same laser damage threshold, PRF improves the power handling capability by at least three orders of magnitude, which is greatly beneficial to both material processing and imaging. For example, the protected silver coating can typically withstand a few hundred mW CW laser power for a 1 μm diameter spot, which is actually close to the power encountered in multiphoton imaging systems, not to mention that the employed sources are femtosecond pulsed lasers.

We utilized the stepwise axial motion in the dual-plane calcium imaging measurement. Depending on the nature of applications, other scanning methods such as curved 3D scanning [22] can also be applied. As all three degrees of freedom are controlled by galvo scanners, monotonic scanning along 3D curves can achieve sub millisecond scanning time.

5. Conclusion

Towards greater power handling capability and avoiding laser damage, we have developed the pupil plane actuated remote focusing. Using tilted objective lenses, we convert the transverse scanning of one lens into the combined axial and transverse scanning of the second lens. Combining PRF with the conventional 2D scanner, we can use three galvo actuators to scan the laser focus in 3D. To evaluate its performance and demonstrate its application, we combined PRF with a two-phonon laser scanning microscope. Using a stepwise axial shift, we implemented the dual-plane *in vivo* calcium recording of the neuronal activity in awake mouse brain. Further development in scanning control is expected to enable more advanced recording methods such as 3D curved scanning, as shown in the initial remote focusing report [22]. PRF can broadly benefit applications that require a few hundred mW or more laser power, especially for systems using energetic laser pulses. As laser scanning is widely employed in imaging and material processing, this development will be valuable to many applications.

Funding

National Institutes of Health (RF1MH120005, U01NS094341, U01NS107689).

Acknowledgment

M.C. acknowledges the scientific equipment from HHMI.

Disclosures

The authors declare no conflicts of interest.

References

1. W. M. Steen and J. Mazumder, *Laser material processing* (springer science & business media, 2010).
2. C. B. Schaffer, A. Brodeur, J. F. García, and E. Mazur, "Micromachining bulk glass by use of femtosecond laser pulses with nanojoule energy," Opt. Lett. **26**(2), 93–95 (2001).
3. T. Duda and L. V. Raghavan, "3D metal printing technology," IFAC-PapersOnLine **49**(29), 103–110 (2016).
4. K. D. Solomon, L. E. F. De Castro, H. P. Sandoval, J. M. Biber, B. Groat, K. D. Neff, M. S. Ying, J. W. French, E. D. Donnenfeld, and R. L. Lindstrom, "LASIK world literature review: quality of life and patient satisfaction," Ophthalmology **116**(4), 691–701 (2009).
5. X. Liu, M. J. Cobb, Y. Chen, M. B. Kimmey, and X. Li, "Rapid-scanning forward-imaging miniature endoscope for real-time optical coherence tomography," Opt. Lett. **29**(15), 1763–1765 (2004).

Optics EXPRESS

6. W. Göbel, B. M. Kampa, and F. Helmchen, "Imaging cellular network dynamics in three dimensions using fast 3D laser scanning," Nat. Methods **4**(1), 73–79 (2007).
7. J. Pawley, *Handbook of Biological Confocal Microscopy*, 3 ed. (Springer, US, 2006).
8. W. Denk and K. Svoboda, "Photon upmanship: Why multiphoton imaging is more than a gimmick," Neuron **18**(3), 351–357 (1997).
9. D. M. Huland, K. Charan, D. G. Ouzounov, J. S. Jones, N. Nishimura, and C. Xu, "Three-photon excited fluorescence imaging of unstained tissue using a GRIN lens endoscope," Biomed. Opt. Express **4**(5), 652–658 (2013).
10. C. Dunsby, "Optically sectioned imaging by oblique plane microscopy," Opt. Express **16**(25), 20306–20316 (2008).
11. M. B. Bouchard, V. Voleti, C. S. Mendes, C. Lacefield, W. B. Grueber, R. S. Mann, R. M. Bruno, and E. M. C. Hillman, "Swept confocally-aligned planar excitation (SCAPE) microscopy for high-speed volumetric imaging of behaving organisms," Nat. Photonics **9**(2), 113–119 (2015).
12. K. F. Tehrani, C. V. Latchoumane, W. M. Southern, E. G. Pendleton, A. Maslesa, L. Karumbaiah, J. A. Call, and L. J. Mortensen, "Five-dimensional two-photon volumetric microscopy of in-vivo dynamic activities using liquid lens remote focusing," Biomed. Opt. Express **10**(7), 3591–3604 (2019).
13. N. Kirkpatrick, E. Chung, D. Cook, X. Han, G. Gruionu, S. Liao, L. Munn, T. Padera, D. Fukumura, and R. K. Jain, "Video-rate resonant scanning multiphoton microscopy: An emerging technique for intravital imaging of the tumor microenvironment," IntraVital **1**(1), 60–68 (2012).
14. T. A. Pologruto, B. L. Sabatini, and K. Svoboda, "ScanImage: flexible software for operating laser scanning microscopes," BioMed Eng OnLine **2**(1), 13 (2003).
15. H. Ren, D. Fox, P. A. Anderson, B. Wu, and S.-T. Wu, "Tunable-focus liquid lens controlled using a servo motor," Opt. Express **14**(18), 8031–8036 (2006).
16. B. F. Grewe, F. F. Voigt, M. van't Hoff, and F. Helmchen, "Fast two-layer two-photon imaging of neuronal cell populations using an electrically tunable lens," Biomed. Opt. Express **2**(7), 2035–2046 (2011).
17. L. Kong, J. Tang, J. P. Little, Y. Yu, T. Laemmermann, C. P. Lin, R. N. Germain, and M. Cui, "Continuous volumetric imaging via an optical phase-locked ultrasound lens," Nat. Methods **12**(8), 759–762 (2015).
18. A. Mermillod-Blondin, E. McLeod, and C. B. Arnold, "High-speed varifocal imaging with a tunable acoustic gradient index of refraction lens," Opt. Lett. **33**(18), 2146–2148 (2008).
19. J.-H. Park, L. Kong, Y. Zhou, and M. Cui, "Large-field-of-view imaging by multi-pupil adaptive optics," Nat. Methods **14**(6), 581–583 (2017).
20. A. Vaziri and V. Emiliani, "Reshaping the optical dimension in optogenetics," Curr. Opin. Neurobiol. **22**(1), 128–137 (2012).
21. S. Shoham, "Optogenetics meets optical wavefront shaping," Nat. Methods **7**(10), 798–799 (2010).
22. E. J. Botcherby, C. W. Smith, M. M. Kohl, D. Debarre, M. J. Booth, R. Juskaitis, O. Paulsen, and T. Wilson, "Aberration-free three-dimensional multiphoton imaging of neuronal activity at kHz rates," Proc. Natl. Acad. Sci. U. S. A. **109**(8), 2919–2924 (2012).
23. E. J. Botcherby, R. Juškaitis, M. J. Booth, and T. Wilson, "An optical technique for remote focusing in microscopy," Opt. Commun. **281**(4), 880–887 (2008).
24. W. Yang, J.-E. K. Miller, L. Carrillo-Reid, E. Pnevmatikakis, L. Paninski, R. Yuste, and D. S. Peterka, "Simultaneous multi-plane imaging of neural circuits," Neuron **89**(2), 269–284 (2016).
25. S. Quirin, D. S. Peterka, and R. Yuste, "Instantaneous three-dimensional sensing using spatial light modulator illumination with extended depth of field imaging," Opt. Express **21**(13), 16007–16021 (2013).
26. M. Dal Maschio, A. M. De Stasi, F. Benfenati, and T. Fellin, "Three-dimensional in vivo scanning microscopy with inertia-free focus control," Opt. Lett. **36**(17), 3503–3505 (2011).
27. R. Liu, N. Ball, J. Brockill, L. Kuan, D. Millman, C. White, A. Leon, D. Williams, S. Nishiwaki, and S. de Vries, "Aberration-free multi-plane imaging of neural activity from the mammalian brain using a fast-switching liquid crystal spatial light modulator," Biomed. Opt. Express **10**(10), 5059–5080 (2019).
28. A. R. Mardinly, I. A. Oldenburg, N. C. Pégard, S. Sridharan, E. H. Lyall, K. Chesnov, S. G. Brohawn, L. Waller, and H. Adesnik, "Precise multimodal optical control of neural ensemble activity," Nat. Neurosci. **21**(6), 881–893 (2018).